

pubs.acs.org/est Article

# Production of Methylmercury in Peatlands Following Permafrost Thaw Increases along a Trophic Gradient

Lauren M. Thompson,\* Renae Shewan, Vaughn Mangal, Lorna I. Harris, Chi Him Cheng, Lucas P. P. Braga, Olesya Kolmakova, Andrew J. Tanentzap, Klaus H. Knorr, McKenzie A. Kuhn, Charlotte Haugk, Alyssa Azaroff, Sofi Jonsson, Vincent L. St. Louis, Igor Lehnherr, William L. Quinton, Oliver Sonnentag, and David Olefeldt\*



Cite This: https://doi.org/10.1021/acs.est.5c04510



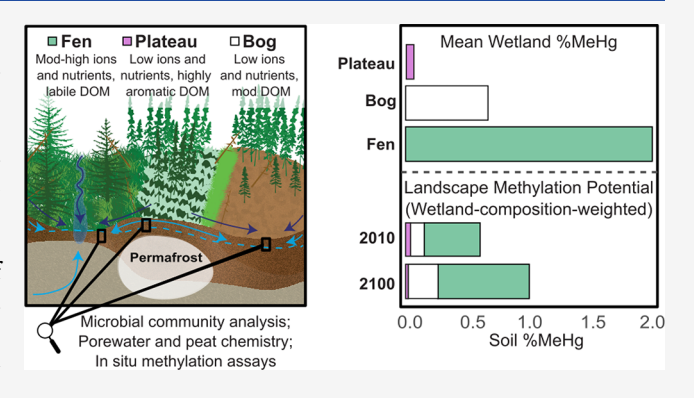
ACCESS

III Metrics & More

Article Recommendations

Supporting Information

ABSTRACT: Permafrost thaw in peatlands risks increasing the production and mobilization of methylmercury (MeHg), a bioaccumulative neurotoxin that poses a health hazard to humans. We studied 12 peatlands on a trophic gradient in northwestern Canada, including permafrost peat plateaus and thawed bogs and fens, to determine the effects of thaw on MeHg production from measures of soil and porewater MeHg and in situ methylation assays. The production of MeHg was greater in thawed peatlands, especially rich fens, as indicated by higher potential rates of microbial methylation of inorganic mercury (Hg) to MeHg and higher soil %MeHg (MeHg:total Hg). Soil %MeHg was 0.1% in permafrost peat plateaus, 0.7% in bogs, and 2.0% in fens. Microbial analysis indicated three putative methylators (two methanogens



and one novel bacteria) as most influential to the community composition, although their abundances were not consistently highest in fens. Fens had a greater range of porewater MeHg concentrations than bogs, potentially due to hydrological flushing, controls on MeHg solubility, or redox disequilibria in fens. MeHg in porewater was strongly associated with dissolved organic matter that had a low aromaticity and a low oxygen-to-carbon ratio. Regionally upscaling our results suggested that the expansion of bogs and fens due to thawing may increase the landscape-scale potential for MeHg production by 65% by 2100, representing a substantial risk to downstream aquatic ecosystems.

KEYWORDS: mercury, soil, porewater, thermokarst wetlands, microbial community, dissolved organic matter, climate change

## **■** INTRODUCTION

Permafrost thaw in northern peatlands causes drastic shifts in land cover and environmental conditions, which may enhance the microbial methylation of inorganic mercury (HgII) to the neurotoxin methylmercury (MeHg). 1,2 In the peatland-rich Taiga Plains of northwestern Canada, recommendations to limit fish consumption from specific species and locations are in place due to elevated mercury (Hg) concentrations driven by MeHg uptake in fish.<sup>3-5</sup> Regional food web studies observed higher concentrations and biomagnification rates of Hg and MeHg in fish in low-relief forested catchments with high dissolved organic matter (DOM) concentrations, <sup>6,7</sup> which are characteristics of peatland-influenced catchments.8 Therefore, understanding changes in MeHg production and transport in peatlands affected by permafrost thaw is essential for northern Indigenous communities that rely on fish as a healthy and culturally significant food source.9

Peatland permafrost thaw in ice-rich discontinuous permafrost causes land surface collapse of peat plateaus with dry surface conditions, leading to the development of thermokarst wetlands with waterlogged, anoxic conditions. <sup>10–12</sup> However, thermokarst wetlands fall on a trophic gradient of nutrient and vegetation species richness, ranging from nutrient-poor bogs to nutrient-poor fens and to nutrient-rich fens, each with varying environmental and water chemistry characteristics that may influence Hg<sup>II</sup> methylation. While thermokarst bogs only receive water and solutes from surrounding raised permafrost peat plateaus and precipitation, fens have variable groundwater connectivity, which leads to higher pH and dissolved ions, depending on groundwater chemistry, and greater processing of DOM than in bogs. <sup>8,13–16</sup> The fens in the Taiga Plains

Received: April 14, 2025 Revised: August 27, 2025 Accepted: August 28, 2025



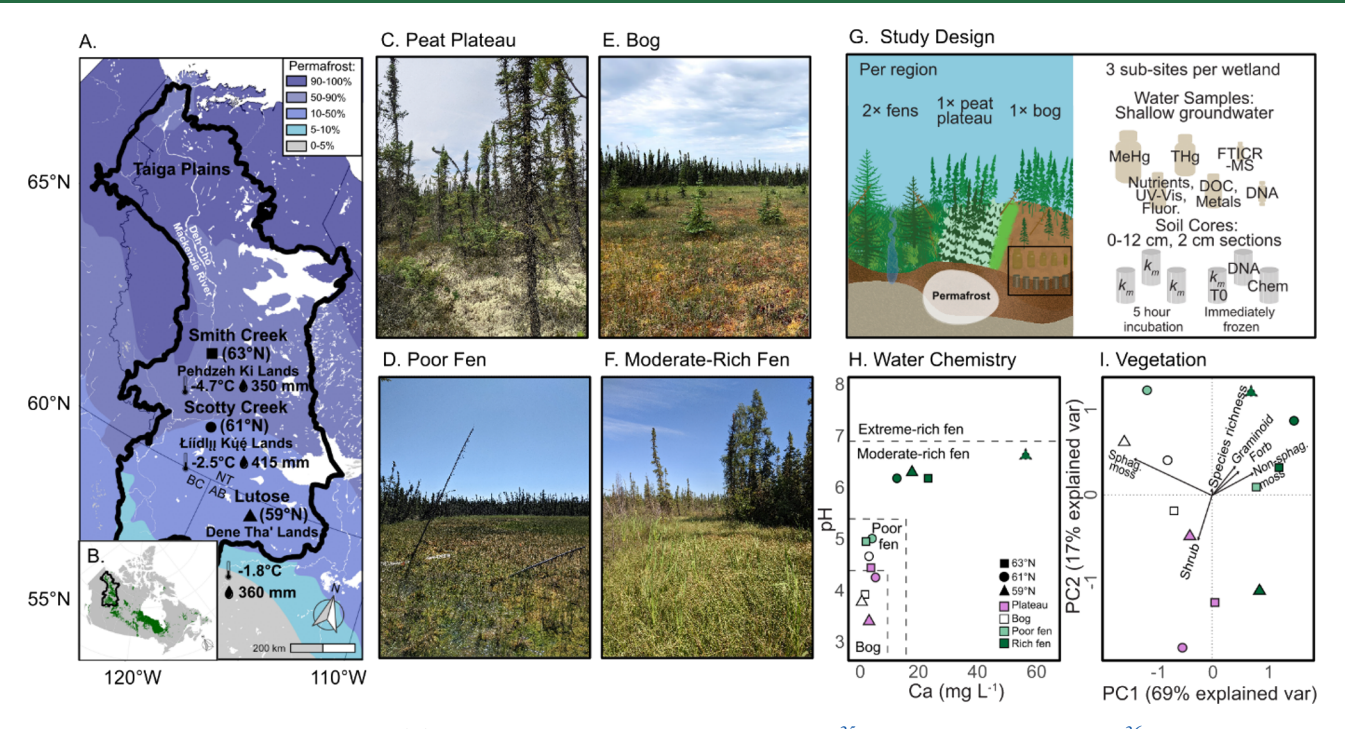


Figure 1. Study sites and sampling design. (A) Study site locations within the Taiga Plains<sup>35</sup> relative to permafrost zones,<sup>36</sup> with mean annual air temperature and total annual precipitation,<sup>37</sup> (B) Taiga Plains region<sup>35</sup> within Canada with an overlay of >25% peatland extent,<sup>38</sup> photographic examples of wetland subsites including (C) peat plateau (63°N), (D) poor fen (63°N), (E) bog (61°N), and (F) moderate-rich fen (59°N) (see satellite imagery of study sites in Table S1), (G) sampling design across regions and wetlands, (H) site classification based on pH and calcium (Ca) where the categories of Ca concentrations are based on a literature review of northern hemisphere peatlands and categories of pH are based on the Alberta Wetland Classification System,<sup>8,39</sup> and (I) principal component analysis (PCA) of vegetation composition. Fens are separated into poor (2) and rich (4) fens, including two rich fens at 59°N, one of which had higher salinity (i.e., Ca,  $SO_4^{2-}$ ) and is indicated by a dashed border. MeHg = methylmercury, THg = total mercury, FTICR-MS = Fourier transform ion cyclotron mass spectrometry, Fluor = fluorescence spectroscopy, DOC = dissolved organic carbon,  $k_m$  = potential Hg<sup>II</sup> methylation rates, chem = soil chemistry. Photos: L. Thompson.

discontinuous permafrost region are also hydrologically well-connected to stream and river networks, while thermokarst bogs are often surrounded by peat plateaus and thus hydrologically isolated.<sup>17</sup>

Hg<sup>II</sup> methylation is known to preferentially occur in anoxic environments with bioavailable Hg<sup>II</sup> and metabolically active anaerobic microbial communities. Terminal electron acceptors (TEAs, i.e., sulfate [SO<sub>4</sub><sup>2-</sup>] or ferric iron [Fe<sup>III</sup>]) and bioavailable organic substrates<sup>18</sup> are required for dissimilatory SO<sub>4</sub><sup>2-</sup> reduction,<sup>19</sup> iron reduction,<sup>20</sup> and methanogenesis.<sup>21,22</sup> Microbes with *hgcAB* genes facilitate Hg<sup>II</sup> methylation, since *hgcA* is a methyl carrier and *hgcB* is an electron donor for corrinoid cofactor reduction.<sup>23</sup> However, specific Hg<sup>II</sup> methylators and their relative contribution to overall methylation are poorly understood for northern peatlands. By targeting *hgcAB* genes through DNA sequencing, it is possible to identify putative Hg<sup>II</sup> methylators within the larger microbial community to understand their relative abundance under various soil environmental conditions.<sup>18</sup>

DOM can both influence Hg<sup>II</sup> methylation and act as a vector for long-range aquatic transport of Hg species, where the concentration and composition of DOM in peatland porewater may act to facilitate or inhibit DOM-Hg<sup>II</sup> complexation, Hg<sup>II</sup> bioavailability, and Hg<sup>II</sup> methylation. High concentrations of aromatic DOM derived from terrigenous sources (i.e., plant matter) tend to be associated with strong complexation and reduced Hg<sup>II</sup> bioavailability.<sup>24–26</sup> Organicmatter-rich peatlands are dominant sources of DOM and cotransported Hg species to streams in boreal regions, <sup>8,27</sup> and the hydrological connectivity between peatland and stream

networks increases with permafrost thaw, with thermokarst fens acting as conduits of water and solutes. <sup>17,28,29</sup> Examining associations between Hg<sup>II</sup> methylation and DOM composition in peatlands with a range of trophic statuses and DOM characteristics can determine the role of DOM as a microbial substrate or a potential vector for MeHg into downstream aquatic ecosystems.

The production and mobilization of MeHg can be inferred using several independent approaches; however, prior studies in Fennoscandia, 10,12 Canada, 11,30-33 and Alaska 13 have predominantly focused on individual lines of evidence to examine different mechanisms and controls within northern ecosystems. Porewater MeHg concentrations reflect MeHg potentially available for transport to downstream ecosystems and can be decoupled from MeHg production, depending on factors that control solubility and transport. 10,11,13,30 Potential  $\mathrm{Hg^{II}}$  methylation rates  $(k_m)$  are a snapshot assessment of short-term MeHg formation that are helpful for site comparisons, although  $k_m$  can vary seasonally  $^{30}$  and can be influenced by the bioavailability of added tracers;  $^{34}$  thus,  $k_m$ rates are suggested to be contextualized by soil MeHg concentrations and soil MeHg to total Hg (THg) ratios (% MeHg), which reflect longer-term net MeHg formation. 12 Additionally, MeHg production is influenced by environmental conditions, the presence of Hg<sup>II</sup> methylators, and potential microbial substrates of TEAs and DOM. Combining methodological approaches is likely to provide synergistic information that will further our understanding of the impacts of permafrost thaw on MeHg production and mobilization in the Taiga Plains, where MeHg dynamics in the region's

peatlands with variable trophic states have not been widely studied.  $^{11,17}$ 

Our study aimed to comprehensively examine how MeHg production is influenced by permafrost thaw, peatland type, and trophic state, building on existing evidence that permafrost thaw enhances MeHg production. We sampled intact permafrost peat plateaus and thawed fens and bogs of the Taiga Plains (>500 km latitudinal gradient, Figure 1) to compare the MeHg and %MeHg of soil and porewater, hgcAB genes, k<sub>m</sub>, TEAs, and DOM composition and concentration. We then utilized data sets of current and future land cover composition in the Taiga Plains for the first effort to quantitatively estimate how climate change will impact landscape-scale Hg<sup>II</sup> methylation potential.

## ■ MATERIALS AND METHODS

**Study Sites.** Samples were collected in July 2021 at three regional peatland sites: Lutose (59°N), Scotty Creek (61°N), and Smith Creek (63°N). The sites span sporadic to extensive discontinuous permafrost zones<sup>36</sup> of western Canada (Figure 1, Table S1) and are located in the homelands of Dene Tha' First Nation, Łiídlų Kų́ę First Nation, and Pehdzeh Ki First Nation, respectively. The study sites have a continental climate with cold winters and short, warm summers, with mean annual air temperatures between -4.7 and -1.8 °C and mean annual precipitation between 350 and 415 mm.<sup>37</sup> These conditions are representative of the Taiga Plains region,<sup>17</sup> which has a mean annual air temperature ranging from -1.0 to -5.1 °C and a mean annual precipitation ranging from 294 to 451 mm, respectively. The study sites are peatland complexes typical of the region,<sup>40,41</sup> comprising a mosaic of intact permafrost peat plateaus and thermokarst wetlands (see satellite imagery in Table S1).

At each regional site, we sampled four wetlands, including one peat plateau (permafrost present) and three permafrostfree wetlands spanning a trophic gradient: one nutrient-poor bog, one nutrient-poor fen, and one nutrient-rich fen (Figure 1). The trophic status of the wetlands (Figure 1) was characterized using porewater pH and calcium (Ca) concentrations.<sup>8,39</sup> We additionally surveyed the presence and percent cover of vegetation in 0.5 m quadrats at four-ten randomly selected locations within each wetland (see Table S2) as a supporting indicator of trophic status and hydrology. Chemistry varied substantially along the trophic gradient (Figure 1H, Figure S1), with the richest fens found at 59°N, likely due to local groundwater discharge; water chemistry classification showed that both fens sampled at 59°N were nutrient-rich fens. Each wetland class had characteristic vegetation composition (Figure 1H), with shrubs and lichen in peat plateaus, bogs dominated by Sphagnum mosses, and fens by brown mosses and graminoids (Table S2).

Our approach focused on near-surface peat and porewater to capture known hotspots of biogeochemical activity. The lability of organic matter and the rate of soil organic matter mineralization have been observed to decrease with depth in peatlands, <sup>42</sup> as does the saturated hydraulic conductivity. <sup>43</sup> As such, it can be expected that microbial activity and the mobility of constituents at depth are reduced relative to the near-surface.

Water Sampling and Analysis. We collected shallow groundwater samples from three subsites per wetland. Soil blocks  $(10 \times 10 \text{ cm})$  were removed from microtopographic hollows to  $\sim 20 \text{ cm}$  depth and allowed to fill with water and

settle from disturbance for ≥1 h. Water for THg and MeHg comprising both dissolved and particulate forms was collected in certified precleaned 125 and 250 mL glass amber bottles (Environmental Supply Company, Inc., Richmond, VA, USA) and preserved with 0.2% and 0.4% trace-metal grade hydrochloric acid (HCl), respectively. THg and MeHg were analyzed at the Canadian Association for Laboratory Accreditation-certified Biogeochemical Analytical Service Laboratory (BASL, University of Alberta) (see S1 in the Supporting Information [SI]). Electrical conductivity (EC) and pH were measured with a calibrated Elite PCTS sensor (Thermo Fisher Scientific, Waltham, MA, USA). Water table position was measured relative to the ground surface at preinstalled wells with a pipe and bubbler at the peat plateaus or measured in the depressions left from the soil blocks (i.e., soil pits) at the fens and bogs.

In each soil pit, we further collected two filtered (0.45  $\mu$ m polyethersulfone membrane; Sartorius AG, Göttingen, Germany) 60 mL water samples in acid-washed amber glass bottles. One sample was acidified with 0.6 mL of 2 M HCl and analyzed for dissolved organic carbon (DOC) and total dissolved nitrogen (TDN) concentrations with a TOC-L combustion analyzer with a TNM-L module (Shimadzu, Japan) at the Natural Resources Analytical Laboratory (University of Alberta). Concentrations of sodium (Na), potassium (K), calcium (Ca), manganese (Mn), iron (Fe), copper (Cu), zinc (Zn), magnesium (Mg), phosphorus (P), and sulfur (S) were also measured from the acidified samples by inductively coupled plasma optical emission spectroscopy (ICP-OES, iCAP6300, Duo, Thermo Fisher Scientific, Waltham, MA, USA). Colorimetry (Thermo Gallery Plus Beermaster Autoanalyzer, Thermo Fisher Scientific, USA) determined the concentrations of chloride (Cl), nitrate-asnitrogen (NO<sub>3</sub>-N), nitrite-as-nitrogen (NO<sub>2</sub>-N), ammoniumas-nitrogen (NH<sub>4</sub>-N), soluble reactive phosphorus (SRP), and sulfate-as-sulfur (SO<sub>4</sub>-S) from the nonacidified samples.

Characterization of DOM composition through UV—vis and fluorescence analysis included the specific UV absorbance at 254 nm (SUVA<sub>254</sub>), the fluorescence index (FI), the humification index (HIX), and the biological index (BIX) (S2, Table S3). We further collected 15 mL of filtered (0.45  $\mu$ m) sample in an acid-washed glass vial, where 5  $\mu$ L of concentrated HCl was added. At the Trent University Water Quality Center, these samples were analyzed for DOM composition with Fourier transform ion cyclotron resonance mass spectrometry (FTICR-MS, see S3). We calculated three FTICR-MS indices, <sup>44,45</sup> including the nominal oxidation state of carbon (NOSC), the modified aromaticity index (AI<sub>mod</sub>), and the double bond equivalence index (DBE) (S3, Table S3). Compounds were also assigned into seven putative classes based on their elemental ratios <sup>46–49</sup> (Table S3).

Water samples for the analysis of microbial communities in porewater were collected by connecting a 0.22  $\mu$ m Sterivex filter (Millipore Sigma, Burlington, MA, USA) to a peristaltic pump and running the pump until the filter was clogged, filtering a minimum of 25 mL. The Sterivex unit was frozen in the field, with analysis details in SI Text S4. A portable freezer unit was kept at -20 °C and accessible within <30 min of sample collection (i.e., in a nearby parked vehicle at 59°N and 63°N and at the research station at 61°N); samples were kept at -20 °C and transferred -80 °C after returning from the field excursion (i.e., within 1-3 weeks).

**Soil Sampling and Analysis.** We collected soil cores for soil chemistry analysis and microbial composition from microtopographic hollows at each subsite using 5 cm diameter Lexan core tubes to a depth of 12 cm. We sampled soils in hollows adjacent to where the porewater was collected. Three separate cores were extracted and segmented at 2 cm intervals, and equivalent depths from each core were combined into sterile Ziplock bags, homogenized, and frozen at  $-20\,^{\circ}\text{C}$  in the field. In the lab, soil samples were dried for 24 h at 55 °C, ground first through a 40-mesh sieve, and then ground to a fine powder using a ball mill (tungsten carbide grinding tools; MM400, Retsch, Germany).

We measured humification through Fourier-transform infrared (FTIR) spectroscopic analysis at the University of Münster, Institute of Landscape Ecology (see S5). We used the R package *irpeat*<sup>50</sup> to compute four humification indices (Table S4). Soil concentrations of carbon (C) and nitrogen (N) were analyzed by catalytic combustion using an elemental analyzer (EA 3000, Eurovector, Italy). Concentrations of other major elements (including Ca, Na, S, and Fe, see S5)<sup>51</sup> were analyzed using wavelength dispersive X-ray fluorescence spectroscopy (WD-XRF; ZSX Primus II, Rigaku, Japan).

In Situ Methylation and Demethylation Assays. We determined potential gross rates of  $Hg^{II}$  methylation  $(k_m)$  and MeHg demethylation  $(k_d)$  by conducting in situ assays of enriched Hg stable-isotope tracers and minimizing disturbances to microbial communities and environmental conditions to the extent possible.<sup>30</sup> Three intact soil cores were collected adjacent to the water sampling and other soil sampling sites from 0 to 12 cm depth with 5 cm diameter Lexan core tubes which had silicone-filled injection ports every 1 cm. Following the protocols by Varty et al., 30 solutions of enriched 198HgII and Me199Hg spike diluted in filtered porewater (0.45  $\mu$ m) and equilibrated for 1 h were injected from the surface at 1 cm intervals from water table depth to 12 cm. Injections added 77.88 ng of 198HgII and 0.257 ng of Me<sup>199</sup>Hg each at 1 cm interval (3.96 ng <sup>198</sup>Hg<sup>II</sup> cm<sup>-3</sup>; 0.013 ng Me<sup>199</sup>Hg cm<sup>-3</sup>). After 5 h of incubation in the extraction hole, 2 cm soil sections were collected, stored in whirl-pack bags, and frozen at −20 °C. A blank soil core was collected alongside the assays, sectioned, bagged, amended with 198HgII and  $\mathrm{Me}^{199}\mathrm{Hg}$  spike, and immediately frozen until analysis at -20°C. Analysis for soil Hg and MeHg is described in SI Text S6.

We used first-order kinetics to calculate  $k_m$  as the proportion of added  $^{198}{\rm Hg^{II}}$  methylated to Me $^{198}{\rm Hg}$ , divided by incubation time (5 h).  $k_d$  was calculated by first-order decay kinetics ( $k_d = -1/t \ln[{\rm MeHg_t/MeHg_0}]$ ), where t is the incubation duration, MeHg0 is the starting concentration, and MeHg1 is the ending concentration. Detection limits for  $k_m$  and  $k_d$  were calculated following Hintelmann and Evans. Soil THg (inorganic + organic Hg) and MeHg concentrations were calculated using the isotopic signal from  $^{202}{\rm Hg^{II}}$  and Me $^{202}{\rm Hg}$  (ambient) concentrations. In addition, a subset of nonspiked soil chemistry samples was analyzed for MeHg concentrations at Stockholm University with methods described by Tarbier et al. Figure S2 shows a strong agreement between the contrasting methods.

**Microbial Analysis.** We used long-read sequencing to characterize the putative Hg-methylating microbes in each subsite (SI Text S4). Sequences were processed according to Thompson et al.<sup>27</sup> Taxonomic classification and abundance profiling were performed based on phylogenetic placements into a gene tree built from curated reference sequences of *hgcA* 

 $(n = 243)^{53}$  using GraftM.<sup>54</sup> Using the Shannon index, we estimated the diversity of Hg methylators in each sample.

Statistical Analyses and Data Visualization. Statistical analyses, including principal component analysis (PCA), redundancy analysis (RDA), analysis of variance (ANOVA, Type II), permutational analysis of variance (permANOVA), and similarity percentage analysis (SIMPER), were performed in RStudio utilizing R version 4.2.055 and the R packages vegan, <sup>56</sup> car, <sup>57</sup> emmeans, <sup>58</sup> and phyloseq <sup>59</sup> (see Table S5 for details). Estimated marginal means (EM<sub>means</sub>) were calculated from each ANOVA model.  $EM_{means}$  are the empirical or theoretical averages extracted from the statistical model for each level of a categorical predictor, averaged across all levels of other predictors (see predictors in Table S5), for example, the means of the response variable (e.g., soil %MeHg) for a specified predictor variable (e.g., Region) across all wetland classes and depths. The results of ANOVA and permANOVA are displayed in Table S6.

We used RDA to assess how wetland characteristics (vegetation composition, water table depth, soil chemistry, water chemistry, and DOM composition) related to  $k_m$ , soil MeHg, and porewater MeHg. In the RDA, the DOM composition was characterized by using the first components in PCA, which included the optical and FTICR-MS indices (Figure S6; Table S7). Where parameters fell below the laboratory detection limits, the detection limit was utilized in the RDA.

We used a van Krevelen diagram to plot the oxygen-to-carbon (O/C) and hydrogen-to-carbon (H/C) ratios of intensity-weighted FTICR-MS-derived molecular formulas, which significantly (p < 0.05) correlated with porewater MeHg concentrations (see SI Text S3).

Estimating Landscape-Scale Methylation in Current and Future Conditions. To project how ongoing permafrost thaw will impact the landscape-scale production of MeHg in the Taiga Plains ecozone, we utilized the Boreal-Arctic Wetland and Lake Data set (BAWLD).<sup>60</sup> BAWLD is a land cover product that differentiates between permafrost and nonpermafrost boreal wetland classes, including current wetland distribution. Scenarios of wetland distribution in 2100 have been projected based on the Shared Socioeconomic Pathway (SSP) SSP2–4.5, which includes scenarios with low, mid, and high rates of thermokarst development.<sup>61</sup>

We harmonized our observations with the BAWLD wetland classes predominant within the Taiga Plains (consistent bog class; fen = inclusion of poor fen and moderate-rich fen; permafrost bog class = peat plateau). We then assessed the current net Hg<sup>II</sup> methylation potential of the landscape. We calculated a representative range (first, second, and third quartiles; Q1, Q2, and Q3) of %MeHg observed in the top 12 cm of soil for each wetland class. For each wetland class, we multiplied the Q1, Q2, and Q3 %MeHg values by their fractional distribution in peatland complexes across the Taiga Plains (ecoregion area from the National Ecological Framework for Canada<sup>62</sup>), both currently and in the future (low, mid, and high thermokarst SSP2–4.5 scenarios). We then summed up the resulting values across wetland classes to produce ranges of landscape-scale estimates of %MeHg.

## ■ RESULTS AND DISCUSSION

MeHg Production Increases in Thermokarst Wetlands. The thermokarst wetlands (i.e., bogs and fens) had higher soil %MeHg (a proxy for net methylation  $^{12,18}$ ),  $k_m$ , soil

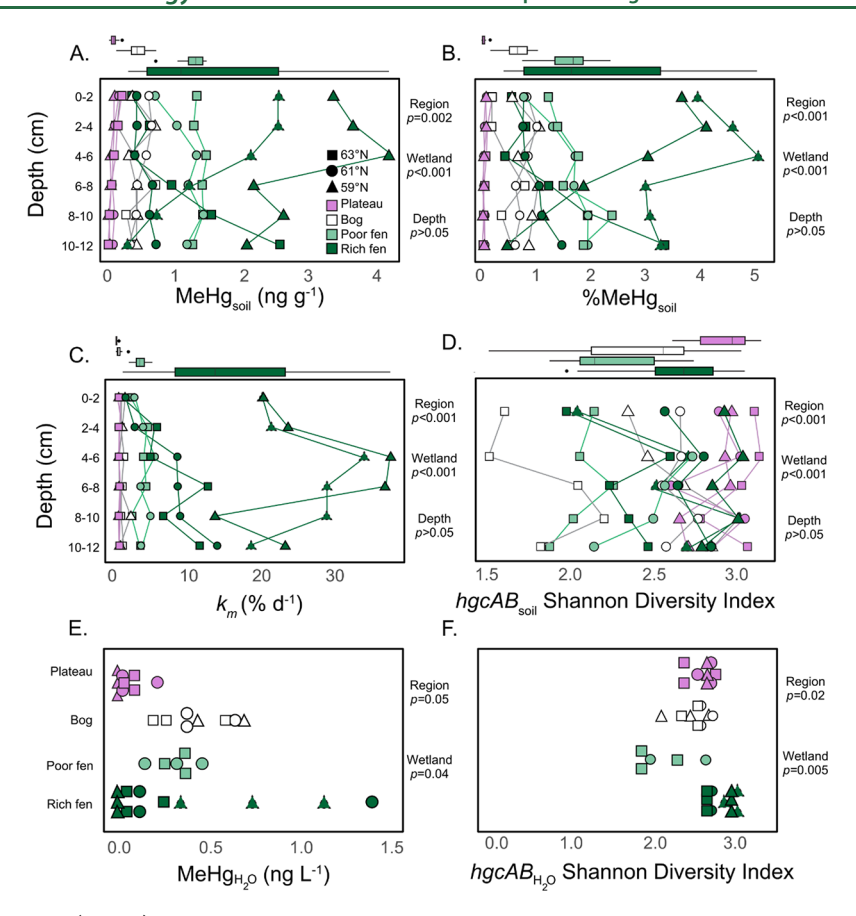


Figure 2. Higher methylmercury (MeHg) in soils and porewaters of thermokarst wetlands compared to that in permafrost peat plateaus. Soil profiles from 0-12 cm depth for (A) concentrations of MeHg, (B) %MeHg (MeHg to total mercury concentration ratio, [MeHg]/[THg]), (C) potential methylation rate  $(k_m)$ , and (D) Shannon diversity index of microbes with hgcAB genes in soils. Soil values are the mean of triplicate samples grouped by the wetland classification. Porewater values of (E) MeHg concentrations and (F) Shannon diversity index of microbes with hgcAB genes in porewater; values are triplicate samples of shallow groundwater, grouped by wetland classification. Fens are separated into poor (2) and rich (4) fens, including two rich fens at  $59^{\circ}$ N, one of which had higher salinity (i.e., Ca,  $SO_4^{2-}$ ) and is indicated by a dashed border. The p-values from testing the region and wetland class variability with ANOVA are displayed beside each plot. For the soil plots, boxplots of the median, first, and third quartiles, whiskers of 1.5 times the interquartile range, and outliers grouped by wetland classification are above each plot. Detailed statistical test results are listed in Table S6.

MeHg concentrations, and lower soil THg concentrations than the peat plateaus (Figure 2; Figure S3A; Table S6A–D). Methylation potential increased with trophic status (plateau < bog < fen), as inferred from soil MeHg concentrations, % MeHg, and  $k_m$ . The EM<sub>means</sub> across all depths and regions showed the contrast between peat plateaus (0.09 ng MeHg g<sup>-1</sup>; 0.06 %MeHg; ~0.08%  $k_m$  d<sup>-1</sup>), bogs (0.44 ng MeHg g<sup>-1</sup>; 0.67 %MeHg; 0.40%  $k_m$  d<sup>-1</sup>), poor fens (1.46 ng MeHg g<sup>-1</sup>; 1.90 %MeHg; 5.90%  $k_m$  d<sup>-1</sup>), and rich fens (1.45 ng MeHg g<sup>-1</sup>; 2.0 %MeHg; 14.62%  $k_m$  d<sup>-1</sup>).

We found that soil MeHg, %MeHg, and  $k_m$  varied significantly among regions and wetland classes, while soil THg varied among regions (Table S6A–D). The fens at 59°N had the highest trophic status (Figure 1), and the highest soil MeHg, %MeHg, and  $k_m$  (Figure 2), which likely drove the differences among regions; the EM<sub>means</sub> at 59°N for those parameters were two or more times higher than 61°N and 63°N (Table S6A,C,D). Only THg concentrations significantly varied with depth in these near-surface samples, with a general decline in concentrations (Figure S3A; mean –24% change from surface [0-2 cm] to base [10-12 cm]). Potential  $k_d$  varied among wetland classes without a clear relation to wetland trophic status (Figure S4A).

We found close agreement between the short-term MeHg production potential  $(k_m)$  and the longer-term balance of net methylation (%MeHg) in soil. Soil  $k_m$  was positively correlated with both soil MeHg concentrations and %MeHg (Figure S5,  $R^2=0.54$  and 0.58, respectively, p<0.001). Although several samples had no detected demethylation,  $k_m/k_d$  patterns among wetland classes also aligned with %MeHg (Figure S4B). Our study showed that the one-time measurements of  $k_m$  using enriched isotopes during the peak summer period (i.e., a snapshot in time) effectively predicted longer-term methylation as indicated by soil %MeHg<sup>18</sup> (Figure S5), despite previous work that showed that  $k_m$  can vary seasonally  $^{30,63}$  and that bioavailability of added isotopes can differ from Hg<sup>II</sup> that is naturally present.  $^{34}$ 

Porewater MeHg concentrations differed significantly among wetland classes (Figure 2E; Table S6E-G), with higher variability and concentrations in thermokarst wetlands than in the peat plateaus. Among thermokarst wetlands, fens exhibited the greatest variability in porewater MeHg, %MeHg, and THg concentrations (Figure 2E; Figure S3B,C).

Although our study did not directly examine the hydrology of the wetlands, one potential driver of more variable porewater MeHg and THg concentrations in fens than bogs is the shorter water residence time and greater groundwater

connectivity in fens. 64,65 While fens support higher soil methylation efficiency (discussed above), porewater MeHg and THg concentrations may be flushed as fens convey water and solutes in their function as the drainage network of peatland complexes (see site imagery in Table S1). The role of fens as conduits for water and solutes was highlighted in a peatland complex in northern Sweden, which identified the lowest DOC concentrations but the highest relative export of DOC in fens compared to palsas (peat mounds underlain by permafrost) and bogs.<sup>29</sup> Flow networks of fens also feed into and out of small peatland lakes or beaver ponds (see site imagery in Table S1), where MeHg photodemethylation, Hg<sup>II</sup> photoreduction, or sedimentation can reduce concentrations.<sup>27,32</sup> Due to the low hydrological connectivity of thermokarst bogs (i.e., many being isolated by surrounding peat plateaus), 17 water has a longer residence time, potentially explaining the greater accumulation of aqueous MeHg and THg. Water in bogs may be stored until removal via evaporation or groundwater recharge; near-surface porewater of bogs only infrequently discharges into channel fens during high flow events. 64 Additional hypotheses for drivers of porewater MeHg variability in thermokarst fens are discussed below.

Geochemical Drivers Related to Trophic Status Control Methylation. Trophic status effectively indicated overall methylation potential as shown in the RDA in Figure 3A, increasing toward the RDA's first axis. Fens were associated with higher concentrations of TEAs, higher pH due to the buffering capacity of carbonate bedrock, greater vegetation species richness, and graminoid cover that supports larger pools of labile DOM<sup>66</sup> (Figure 3A). Peat plateaus had lower pH and lower TEA concentrations, higher soil carbon-to-nitrogen ratios, and higher concentrations of DOC with more aromatic quality. Bogs fell between the fens and plateaus.

Higher potential  $k_m$  was associated with higher concentrations of SO<sub>4</sub>-S and Fe in porewater (Figure 3A). The presence of  $SO_4^{\ 2-}$  and Fe can control  $Hg^{II}$  methylation as fuel for methylating microbes<sup>18</sup> and can influence MeHg solubility. Solubility. Solubility. We observed the highest  $k_m$  values at the 59°N rich fens (Figure 2C), which had distinct water chemistry driven by groundwater inputs due to surrounding high-elevation areas and sporadic permafrost cover that permits subsurface flow paths. One fen had the highest porewater  $SO_4^{2-}$  (13.7 mg  $SO_4$ -S L<sup>-1</sup>) and soil S (7.4 mg S  $g_{-1}$ ), and the other fen had the highest porewater and soil iron (0.56 mg Fe L<sup>-1</sup>; 5.6 mg Fe g<sup>-1</sup>) but nondetectable porewater SO<sub>4</sub><sup>2-</sup>. The conditions of the high SO<sub>4</sub><sup>2-</sup> rich fen were an outlier with positive RDA1 and RDA2 loadings, while the low SO<sub>4</sub><sup>2-</sup> rich fen was more representative and clustered with the rich fens at 61°N and 63°N with positive RDA1 loadings and negative RDA2 loadings (Figure 3A). Although both rich fens at 59°N had high  $k_m$  values and soil MeHg concentrations (Figure 2C; Figure 2A), the high  $SO_4^{2-}$  rich fen had relatively high porewater MeHg concentrations, while the low SO<sub>4</sub><sup>2-</sup> rich fen had among the lowest porewater MeHg concentrations (Figure 2E). We suggest that controls on MeHg solubility are another potential driver of the variability in porewater MeHg concentrations in thermokarst fens. For example, additions of  $SO_4^{\ 2-}$  in peatlands have been associated with enhanced MeHg production from increased bioavailability of  $Hg^{II}$  due to the formation of neutral Hg-sulfides produced by SO<sub>4</sub><sup>2-</sup> reduction, as well as enhanced MeHg solubility. This solubility influence may explain the

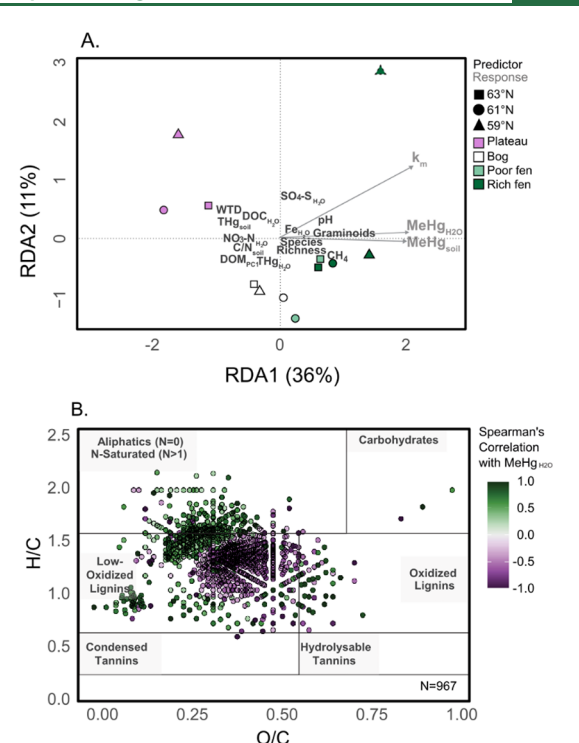


Figure 3. Influence of wetland biogeochemistry and dissolved organic matter (DOM) composition on methylmercury (MeHg) concentrations and the inorganic mercury (HgII) methylation potential. (A) Redundancy analysis (RDA) ordination for MeHg concentrations in soil and porewater, as well as potential methylation rates  $(k_m)$  in soil. Predictors include water table depth (WTD), dissolved organic carbon (DOC), PC1 scores from a PCA of dissolved organic matter indices (DOM<sub>PC1</sub>; Figure S6), total mercury (THg), methane flux (CH<sub>4</sub>; Table S8; Harris et al.<sup>67</sup>), carbon to nitrogen ratio (C/N), nitrate-as-nitrogen (NO<sub>3</sub>-N), sulfate-as-sulfur (SO<sub>4</sub>-S), iron (Fe), pH, vegetation species richness, and percent graminoid cover (graminoids). Subscripts indicate whether the parameter was measured in soil or porewater (H2O). Fens are separated into poor (2) and rich (4) fens, including two rich fens at 59°N, one of which had higher salinity (i.e., Ca, SO<sub>4</sub><sup>2-</sup>) and is indicated by a dashed border. (B) Relationships between putative DOM compound classes (denoted by boxed regions<sup>46</sup>) and MeHg concentrations in wetland porewaters. Van Krevelen plot of oxygen/carbon (O/C) and hydrogen/carbon (H/C) wherein each data point represents the strength of significant correlations (Spearman's Rank, p < 0.05 after 999 permutations) between the relative intensity of a specific DOM formula and porewater MeHg concentrations in each sample.

coherence in high  $k_m$  and high soil and porewater MeHg concentrations at the high  ${\rm SO_4}^{2-}$  rich fen and the disconnect between soil MeHg and porewater MeHg at the low  ${\rm SO_4}^{2-}$  rich fen.

Wetlands with higher porewater and soil MeHg concentrations also had higher methane emissions (measured concurrently via chamber fluxes at each wetland;<sup>67</sup> Table S8; Figure 3A). The activity of methanogens and syntrophs (i.e., between secondary fermenters and methanogens) is a pathway of mineralizing organic matter via fermentation products and can mediate MeHg production under reducing conditions with depletion of more energetically favorable TEAs.<sup>69</sup> The link between MeHg production and methane emissions has also been observed in Arctic ponds,<sup>31</sup> rivers,<sup>70</sup> and soils.<sup>71</sup> However, high methane emissions were not universally associated with high soil and porewater MeHg concentrations; the high SO<sub>4</sub><sup>2-</sup> fen at 59°N had relatively low methane

emissions (Table S8), likely due to  ${\rm SO_4}^{2^-}$ -reducing bacteria outcompeting methanogens. Higher porewater and soil MeHg concentrations were also associated with abundant graminoid vegetation species, greater vegetation species richness, and a shallower water table depth (Figure 3A). However, the presence of vascular plants and associated oxygen shuttling in aerenchyma tissues can result in heterogeneous redox conditions in wetlands 66,73,74 and regeneration of TEAs, potentially enhancing MeHg production through pathways other than methanogenesis (i.e.,  $SO_4^{2-}$ reduction or iron reduction). These heterogeneous redox conditions may contribute to the local variability of porewater MeHg concentrations in the rich fens. In the drier peat plateaus, homogeneous oxygen availability was a likely factor in dampening the activity of methylating microbes, 18 and we observed lower porewater MeHg concentrations, soil MeHg concentrations, and  $k_m$  relative to the thermokarst wetlands (Figures 2 and 3A).

Porewater MeHg concentrations increased with the relative abundance of nonaromatic and higher H/C DOM, suggesting that bioavailable DOM may have facilitated HgII methylation (Figure 3B). Characteristic of peatlands, DOC concentrations were generally high (Figure S1, range: 26 to 93 mg DOC  $L^{-1}$ ). We found that higher porewater MeHg concentrations were associated with lower DOC concentrations but also lower DOC aromaticity (Figure 3A). From the van Krevelen diagram (Figure 3B), we found generally positive correlations between MeHg concentrations and the relative abundance of formulas with high H/C and low O/C and negative correlations between MeHg concentrations and the relative abundance of formulas with lower H/C and higher O/C formulas (Figure 3B). We observed rich fens to have relatively more fresher and microbially derived DOM (Figure S1, Figure S6), potentially more labile and thus fueling MeHg production and enhancing Hg<sup>II</sup> bioavailability. <sup>24,25,75</sup> Greater DOM processing typically occurs in fens, <sup>8,29,76</sup> and vascular plants such as graminoids can deliver labile DOM through root exudates.66 MeHg production was previously observed to associate with bioavailable DOM in boreal lakes<sup>25,75,77</sup> and peatlands.<sup>74</sup> The strong correlation between MeHg and fresh, microbially derived, and nonaromatic DOM in this study contrasts with observations from streams and rivers, where MeHg has more often been associated with aromatic DOM. This discrepancy is likely driven by aromatic DOM acting as a vector to facilitate the cotransport of MeHg as shown in streams draining the studied wetlands<sup>27,78</sup> and in other boreal streams.<sup>26,79</sup>

The striking association between MeHg concentrations in porewater and DOM likely to be bioavailable could also be driven by the generally anoxic conditions in the fens, independently enhancing methylation and enriching labile DOM. Under reducing conditions, anaerobic microbes preferentially consume compounds with high NOSC values, leading to the enrichment of low NOSC substrates.<sup>80,81</sup> The DOM compounds in the higher H/C and lower O/C regions had lower NOSC values, as did richer fens (Figure S7). Therefore, the DOM may not solely represent a substrate for Hg<sup>II</sup> methylation, with a low NOSC DOM potentially reflecting the result of processing under reducing conditions. The correlation between porewater MeHg concentrations and DOM representative of processing under reducing conditions in these regions could instead suggest that the predominantly reducing conditions are the driver of higher overall MeHg production and solubility in wetlands.

Diversity and Composition of Putative Methylators. Our results implicated a small number of putative Hg methylators as primary contributors to the differences in community composition. Using permANOVA, we found that the composition of putative methylators varied significantly among wetland classes in porewaters ( $R^2 = 0.56$ , p = 0.001, Table S6I) and soils ( $R^2 = 0.16$ , p = 0.001, Table S6H) and among regional sites in soil ( $R^2 = 0.08$ , p = 0.010, Table S6H). With SIMPER analysis, we specifically identified three taxa that had the greatest cumulative contributions to differences in the community composition of methylators in soils (39%): one resolved to the genus Methanoregula, one novel bacteria (i.e., was not resolved past classification of bacteria, a common issue when identifying putative methylators<sup>18</sup>), and one resolved to the genus Methanocella. In porewater, two taxa (from the genus Methanoregula and the novel bacteria) had the greatest cumulative contributions in porewater (29%). Both methanogen genera (Methanoregula, Methanocella) were identified previously as putative methylators, with in-culture methylation ability confirmed in Methanocella paludicola SANAE. 82 With methanogens present as key putative methylators and MeHg concentrations linked with methane emissions within the RDA, the consequence of permafrost thaw leading to anoxic and reducing conditions has the potential to synergistically enhance

both methane emissions and MeHg production in the region.

Abundances of the three taxa that are important for explaining methylator community composition were generally congruent in soils and porewater. Methanoregula abundance varied among wetland classes and regional sites in soils (p < p)0.001 and p = 0.01, respectively, Table S6L) and among wetland classes in porewater (p < 0.001, Table S6M); Methanoregula had the highest abundance in poor fens for both soils and porewater (see EM<sub>means</sub> in Table S6L, Table S6M). The abundance of the novel bacteria likewise varied among wetland classes and regional sites in soils (p = 0.05 and p = 0.001, respectively, Table S6N) and among wetland classes in porewater (p = 0.002, Table S6O). Rich fens and plateaus had the highest abundances of the novel bacteria in soils and porewater (Table S6O, Table S6N). Abundances of Methanocella in soils varied by wetland class and regional sites (p =0.04 and p < 0.001, respectively, Table S6P), with the highest abundances in bogs and rich fens (Table S6P). Overall, the highest abundances of influential taxa were not consistently found in the fens, which we identified as having the highest Hg<sup>II</sup> methylation potential. Additionally, a higher diversity of putative methylators was not observed in porewaters or soil of thermokarst wetlands relative to plateaus (Figure 2D; Figure 2F; Table S6K; Table S6J). Our results align with previous studies that found that the presence of putative methylators does not necessarily reflect their activity due to factors such as HgII bioavailability or the availability of electron donors and acceptors. 18,83

Effects of Continued Permafrost Thaw on Near-Surface Hg<sup>II</sup> Methylation Capacity at a Landscape Scale. The landscape composition of the Taiga Plains is expected to undergo continued changes due to permafrost thawing, which may lead to an enhanced production of MeHg on a landscape scale. In the Taiga Plains, fens are the predominant wetland type that form after permafrost thaw, enhancing hydrological connectivity within catchments and transporting water and solutes to downstream aquatic systems. 64,65 Additionally, the thawing of peat plateaus can reduce subsurface hydrogeological barriers, leading to the

drainage of previously isolated bogs and activating subsurface pathways for nutrient and ion delivery through groundwater discharge. Our data indicate that thermokarst bogs and fens are sites of higher MeHg production compared with intact permafrost peat plateaus within the Taiga Plains of northwestern Canada. The highest concentrations of MeHg and potential Hg<sup>II</sup> methylation rates were associated with fens that were enriched in nutrients and labile DOM, located within the southernmost regional sites.

Landcover composition served as the foundation for estimating current and future landscape HgII methylation potential (i.e., representative %MeHg per soil class multiplied by its fractional distribution in peatland complexes across the Taiga Plains; see methods). In the BAWLD land cover product,60 peatland complexes across the Taiga Plains are currently composed of 61% peat plateaus, 17% bogs, and 23% fens (Table S9). By 2100, with continued permafrost thaw, the distribution of peatland complexes is expected to shift due to widespread losses of peat plateaus (reduced to 28% cover) and subsequent expansion of bogs (increased to 35% cover) and fens (increased to 37% cover) under a SSP2-4.5 midthermokarst scenario<sup>61</sup> (Table S9). While our upscaling considers shifts in the relative composition of plateaus, bogs, and fens in the Taiga Plains, we acknowledge that MeHg production is likely to be further affected by additional environmental factors, such as soil temperature, 71 water table fluctuations,<sup>66</sup> and wildfire activity.<sup>84</sup>

Given the projected thaw of permafrost peat plateaus and expansion of bogs and fens across the Taiga Plains, we anticipate increases of 65% (range: 47–80%) in the average peatland landscape %MeHg of near-surface soils (Table S9; percent change from Q2 of current %MeHg versus low, mid, high scenarios). The %MeHg decreases in peat plateaus (–50%, –75% to –25%) and increases in bogs (+118%, +80% to +145%) and fens (+62%, +47 to +78%). By taking %MeHg as a proxy for landscape-scale net methylation, we see an apparent effect of permafrost thaw leading to enhanced Hg<sup>II</sup> methylation potential across the landscape of northwestern Canada by 2100. Increased Hg<sup>II</sup> methylation, coupled with greater landscape connectivity due to thaw, may further lead to enhanced cotransport of DOM with MeHg in downstream environments, increasing risks to human well-being.

## ASSOCIATED CONTENT

## **Data Availability Statement**

University of Alberta Education & Research Archive hosts the soil and porewater chemistry data (10.7939/r3-vp5e-aj53). The *hgcAB* sequencing data are available in the Sequence Read Archive (https://www.ncbi.nlm.nih.gov/sra) under the ID PRJNA1036607. The Boreal-Arctic Wetland and Lake Data set (BAWLD) is accessible from the Arctic Data Center (https://arcticdata.io/catalog/view/doi:10.18739/A2C824F9X), with the Taiga Plains boundaries accessed from the National Ecological Framework for Canada (https://sis.agr.gc.ca/cansis/nsdb/ecostrat/gis\_data.html).

## Supporting Information

The Supporting Information is available free of charge at https://pubs.acs.org/doi/10.1021/acs.est.5c04510.

Supplemental text on Hg and MeHg analysis in water (S1), DOM optical analysis in water (S2), FTICR-MS analysis in water (S3), microbial analysis in soil and water (S4), elemental and FTIR analysis in soil (S5), Hg

and MeHg analysis in soil (S6); Supporting figures of geochemistry and organic matter composition of porewater and soil (Figure S1), comparison of MeHg concentrations in soil with different analysis methods (Figure S2), concentrations of total Hg in porewater and soil and MeHg:total Hg in porewater (Figure S3), soil potential demethylation rates (Figure S4), correlations between MeHg in soil and MeHg:total Hg in soil versus potential methylation rates (Figure S5), principal component analysis of DOM indices (Figure S6), NOSC in porewater (Figure S7); Supporting tables of characteristics of each sampling region (Table S1), species list for vegetation of sampled wetlands (Table S2), DOM indices (Table S3), soil humification indices (Table S4), details on statistical methods (Table S5), results of ANOVA and PermANOVA analysis (Table S6), principal component analysis loadings (Table S7), methane flux concurrently measured (Table S8), and projections of landscape methylation (Table S9) (PDF)

# ■ AUTHOR INFORMATION

# **Corresponding Authors**

Lauren M. Thompson — Department of Renewable Resources, University of Alberta, Edmonton, AB T6G 2R3, Canada; orcid.org/0000-0002-6455-4980;

Email: lauren.thompson@ualberta.ca

David Olefeldt — Department of Renewable Resources, University of Alberta, Edmonton, AB T6G 2R3, Canada; Email: olefeldt@ualberta.ca

## Authors

Renae Shewan – Department of Renewable Resources, University of Alberta, Edmonton, AB T6G 2R3, Canada

Vaughn Mangal – Department of Chemistry, Brock University, St. Catharines, ON L2S 3A1, Canada

Lorna I. Harris – Department of Renewable Resources, University of Alberta, Edmonton, AB T6G 2R3, Canada

Chi Him Cheng – Ecosystems and Global Change Group, Department of Plant Sciences, University of Cambridge, Cambridge CB2 3EA, England

Lucas P. P. Braga – Ecosystems and Global Change Group, Department of Plant Sciences, University of Cambridge, Cambridge CB2 3EA, England

Olesya Kolmakova — Ecosystems and Global Change Group, Department of Plant Sciences, University of Cambridge, Cambridge CB2 3EA, England

Andrew J. Tanentzap — Ecosystems and Global Change Group, Department of Plant Sciences, University of Cambridge, Cambridge CB2 3EA, England; Ecosystems and Global Change Group, School of Environment, Trent University, Peterborough, ON K9L 0G2, Canada

Klaus H. Knorr — Ecohydrology & Biogeochemistry Group, Institute of Landscape Ecology, University of Münster, Münster 48149, Germany; orcid.org/0000-0003-4175-0214

McKenzie A. Kuhn – Department of Geography, University of British Columbia, Vancouver, BC V6T 1Z2, Canada

Charlotte Haugk – Department of Environmental Science, Stockholm University, Stockholm SE-106 91, Sweden

Alyssa Azaroff – Department of Environmental Science, Stockholm University, Stockholm SE-106 91, Sweden Sofi Jonsson – Department of Environmental Science,

Sofi Jonsson – Department of Environmental Science, Stockholm University, Stockholm SE-106 91, Sweden

- Vincent L. St. Louis Department of Biological Sciences, University of Alberta, Edmonton, AB T6G 2H5, Canada Igor Lehnherr — Department of Geography, Geomatics and Environment, University of Toronto Mississauga, Mississauga, ON L5L 1C6, Canada; ⊚ orcid.org/0000-0002-4618-7128
- William L. Quinton Department of Geography and Environmental Studies, Wilfrid Laurier University, Waterloo, ON N2L 3G1, Canada
- Oliver Sonnentag Département de Géographie, Université de Montréal, Montreal, QC H2 V 0B3, Canada

Complete contact information is available at: https://pubs.acs.org/10.1021/acs.est.5c04510

#### Notes

The authors declare no competing financial interest.

## ACKNOWLEDGMENTS

Research for this publication was undertaken on the lands and territories of Treaty 11, 8, and 6 of contemporary Canada. We are grateful for analytical support from Mingsheng Ma, Yuting (Tina) Chen, Wendong (Neil) Liu, Crystal Dodge, Meng (Athena) Yun Hua, Allan Harms, Yi Zhang, Henning Teickner, Jonas Kurth, and Daniel Brüggemann, as well as field support from Kate Marouelli, and Christopher Schulze and the team from the Scotty Creek Research Station including Mason Dominico, Maude Auclair, and Iain Thomson. Thank you to Kyra St. Pierre for assistance with the study methods and design. Funding for this study was provided by the Campus Alberta Innovates Program to DO, NWT Cumulative Impact Monitoring Program (CIMP199) to D.O. and O.S., Fonds de recherche du Québec Nature et technologies to O.S., Natural Sciences and Engineering Research Council (Alliance Grant ALLRP 555925-20 to W.L.Q., D.O., O.S.; Discovery Grant RGPIN-2016-04688 to D.O.; CGS-M to L.M.T.; PGS-D to L.M.T.), Horizon 2020 European Research Council Starting Grant (804673, sEEIngDOM to A.J.T.), Canada Research Chair program to O.S., Dehcho-AAROM, Weston Family Foundation to L.M.T., Northern Scientific Training Program to L.M.T., and University of Alberta Northern Research Award to L.M.T.

# **■** REFERENCES

- (1) Malcata Martins, B.; Hintelmann, H.; Pilote, M.; Vieira, G.; Canário, J. Recent Advances in the Study of Mercury Biogeochemistry in Arctic Permafrost Ecosystems. *Sci. Total Environ.* **2025**, 959, No. 178176.
- (2) Jonsson, S.; Mastromonaco, M. N.; Wang, F.; Bravo, A. G.; Cairns, W. R. L.; Chételat, J.; Douglas, T. A.; Lescord, G.; Ukonmaanaho, L.; Heimbürger-Boavida, L.-E. Arctic Methylmercury Cycling. *Sci. Total Environ.* **2022**, *850*, No. 157445.
- (3) Government of the Northwest Territories. Site Specific Fish Consumption Advice. https://www.hss.gov.nt.ca/en/services/fish-consumption-guidance/site-specific-fish-consumption-advice (accessed 2025–07–10).
- (4) Government of Alberta. Fish Consumption Guidance: Mercury in Fish.; Environmental Public Health Science Unit, Health Protection Branch, Public Health and Compliance Division, Alberta Health. Edmonton, Alberta.: Edmonton, Alberta, 2019.
- (5) Skinner, K.; Ratelle, M.; Brandow, D.; Furgal, C.; Boyd, A.; Laird, B. Awareness and Perceptions of Contaminants in the Dehcho and Sahtú Regions of the Northwest Territories. *Int. J. Circumpolar Health* **2024**, *83* (1), No. 2387381.
- (6) Moslemi-Aqdam, M.; Low, G.; Low, M.; Laird, B. D.; Branfireun, B. A.; Swanson, H. K. Estimates, Spatial Variability, and Environ-

- mental Drivers of Mercury Biomagnification Rates through Lake Food Webs in the Canadian Subarctic. *Environ. Res.* **2023**, *217*, No. 114835.
- (7) Moslemi-Aqdam, M.; Baker, L. F.; Baltzer, J. L.; Branfireun, B. A.; Evans, M. S.; Laird, B. D.; Low, G.; Low, M.; Swanson, H. K. Understanding Among-Lake Variability of Mercury Concentrations in Northern Pike (Esox Lucius): A Whole-Ecosystem Study in Subarctic Lakes. *Sci. Total Environ.* **2022**, *822*, No. 153430.
- (8) Bourbonniere, R. A. Review of Water Chemistry Research in Natural and Disturbed Peatlands. *Can. Water Resour. J.* **2009**, 34 (4), 393–414.
- (9) Basu, N.; Abass, K.; Dietz, R.; Krümmel, E.; Rautio, A.; Weihe, P. The Impact of Mercury Contamination on Human Health in the Arctic: A State of the Science Review. *Sci. Total Environ.* **2022**, *831*, No. 154793.
- (10) Fahnestock, M. F.; Bryce, J. G.; McCalley, C. K.; Montesdeoca, M.; Bai, S.; Li, Y.; Driscoll, C. T.; Crill, P. M.; Rich, V. I.; Varner, R. K. Mercury Reallocation in Thawing Subarctic Peatlands. *Geochem. Persp. Lett.* **2019**, 33–38.
- (11) Gordon, J.; Quinton, W.; Branfireun, B. A.; Olefeldt, D. Mercury and Methylmercury Biogeochemistry in a Thawing Permafrost Wetland Complex, Northwest Territories. *Canada. Hydrol. Process.* **2016**, 30 (20), 3627–3638.
- (12) Tarbier, B.; Hugelius, G.; Kristina Sannel, A. B.; Baptista-Salazar, C.; Jonsson, S. Permafrost Thaw Increases Methylmercury Formation in Subarctic Fennoscandia. *Environ. Sci. Technol.* **2021**, *55* (10), 6710–6717.
- (13) Poulin, B. A.; Ryan, J. N.; Tate, M. T.; Krabbenhoft, D. P.; Hines, M. E.; Barkay, T.; Schaefer, J.; Aiken, G. R. Geochemical Factors Controlling Dissolved Elemental Mercury and Methylmercury Formation in Alaskan Wetlands of Varying Trophic Status. *Environ. Sci. Technol.* **2019**, *53* (11), 6203–6213.
- (14) Vitt, D. H.; Chee, W.-L. The Relationships of Vegetation to Surface Water Chemistry and Peat Chemistry in Fens of Alberta. *Canada. Vegetatio* **1990**, 89 (2), 87–106.
- (15) Olefeldt, D.; Roulet, N. T. Permafrost Conditions in Peatlands Regulate Magnitude, Timing, and Chemical Composition of Catchment Dissolved Organic Carbon Export. *Glob. Change Biol.* **2014**, *20* (10), 3122–3136.
- (16) Folhas, D.; Couture, R.-M.; Laurion, I.; Vieira, G.; Canário, J. Natural Organic Matter Dynamics in Permafrost Peatlands: Critical Overview of Recent Findings and Characterization Tools. *Trends Anal. Chem.* **2025**, *184*, No. 118153.
- (17) Wright, S. N.; Thompson, L. M.; Olefeldt, D.; Connon, R. F.; Carpino, O. A.; Beel, C. R.; Quinton, W. L. Thaw-Induced Impacts on Land and Water in Discontinuous Permafrost: A Review of the Taiga Plains and Taiga Shield. *Northwestern Canada. Earth-Sci. Rev.* 2022, 232. No. 104104.
- (18) Bravo, A. G.; Cosio, C. Biotic Formation of Methylmercury: A Bio-Physico-Chemical Conundrum. *Limnol. Oceanogr.* **2020**, *65* (5), 1010–1027.
- (19) Gilmour, C. C.; Henry, E. A.; Mitchell, R. Sulfate Stimulation of Mercury Methylation in Freshwater Sediments. *Environ. Sci. Technol.* **1992**, *26* (11), 2281–2287.
- (20) Fleming, E. J.; Mack, E. E.; Green, P. G.; Nelson, D. C. Mercury Methylation from Unexpected Sources: Molybdate-Inhibited Freshwater Sediments and an Iron-Reducing Bacterium. *Appl. Environ. Microbiol.* **2006**, 72 (1), 457–464.
- (21) Gilmour, C. C.; Podar, M.; Bullock, A. L.; Graham, A. M.; Brown, S. D.; Somenahally, A. C.; Johs, A.; Hurt, R. A.; Bailey, K. L.; Elias, D. A. Mercury Methylation by Novel Microorganisms from New Environments. *Environ. Sci. Technol.* **2013**, 47 (20), 11810–11820.
- (22) Hamelin, S.; Amyot, M.; Barkay, T.; Wang, Y.; Planas, D. Methanogens: Principal Methylators of Mercury in Lake Periphyton. *Environ. Sci. Technol.* **2011**, 45 (18), 7693–7700.
- (23) Parks, J. M.; Johs, A.; Podar, M.; Bridou, R.; Hurt, R. A.; Smith, S. D.; Tomanicek, S. J.; Qian, Y.; Brown, S. D.; Brandt, C. C.; Palumbo, A. V.; Smith, J. C.; Wall, J. D.; Elias, D. A.; Liang, L. The

- Genetic Basis for Bacterial Mercury Methylation. *Science* **2013**, 339 (6125), 1332–1335.
- (24) Chiasson-Gould, S. A.; Blais, J. M.; Poulain, A. J. Dissolved Organic Matter Kinetically Controls Mercury Bioavailability to Bacteria. *Environ. Sci. Technol.* **2014**, *48* (6), 3153–3161.
- (25) Bravo, A. G.; Bouchet, S.; Tolu, J.; Björn, E.; Mateos-Rivera, A.; Bertilsson, S. Molecular Composition of Organic Matter Controls Methylmercury Formation in Boreal Lakes. *Nat. Commun.* **2017**, 8 (1), No. 14255.
- (26) Mangal, V.; Lam, W. Y.; Huang, H.; Emilson, E. J. S.; Mackereth, R. W.; Mitchell, C. P. J. Molecular Correlations of Dissolved Organic Matter with Inorganic Mercury and Methylmercury in Canadian Boreal Streams. *Biogeochemistry* **2022**, *160* (1), 127–144.
- (27) Thompson, L. M.; Kuhn, M. A.; Winder, J. C.; Braga, L. P. P.; Hutchins, R. H. S.; Tanentzap, A. J.; St. Louis, V. L.; Olefeldt, D. Controls on Methylmercury Concentrations in Lakes and Streams of Peatland-rich Catchments along a 1700 km Permafrost Gradient. *Limnol. Oceanogr.* 2023, 68, 583–597.
- (28) Connon, R. F.; Quinton, W. L.; Craig, J. R.; Hayashi, M. Changing Hydrologic Connectivity Due to Permafrost Thaw in the Lower Liard River Valley, NWT. *Canada. Hydrol. Process.* **2014**, 28 (14), 4163–4178.
- (29) Olefeldt, D.; Roulet, N.; Giesler, R.; Persson, A. Total Waterborne Carbon Export and DOC Composition from Ten Nested Subarctic Peatland Catchments-Importance of Peatland Cover, Groundwater Influence, and Inter-Annual Variability of Precipitation Patterns. *Hydrol. Process.* **2013**, 27 (16), 2280–2294.
- (30) Varty, S.; Lehnherr, I.; St. Pierre, K.; Kirk, J.; Wisniewski, V. Methylmercury Transport and Fate Shows Strong Seasonal and Spatial Variability along a High Arctic Freshwater Hydrologic Continuum. *Environ. Sci. Technol.* **2021**, *55* (1), 331–340.
- (31) Lehnherr, I.; St. Louis, V. L.; Kirk, J. L. Methylmercury Cycling in High Arctic Wetland Ponds: Controls on Sedimentary Production. *Environ. Sci. Technol.* **2012**, *46* (19), 10523–10531.
- (32) Lehnherr, I.; St. Louis, V. L.; Emmerton, C. A.; Barker, J. D.; Kirk, J. L. Methylmercury Cycling in High Arctic Wetland Ponds: Sources and Sinks. *Environ. Sci. Technol.* **2012**, *46* (19), 10514–10522.
- (33) Cardinal, R.-M.; Roy-Léveillée, P.; Gauthier, S.; Branfireun, B. Methylmercury Concentrations in a Degrading Lithalsa Field: Effects of Thermokarst Development and Revegetation. *Sci. Total Environ.* **2025**, *976*, No. 179276.
- (34) Jonsson, S.; Skyllberg, U.; Nilsson, M. B.; Westlund, P.-O.; Shchukarev, A.; Lundberg, E.; Björn, E. Mercury Methylation Rates for Geochemically Relevant Hg II Species in Sediments. *Environ. Sci. Technol.* **2012**, *46* (21), 11653–11659.
- (35) Agriculture and Agri-Food Canada. *National Ecological Framework for Canada GIS Data, Ecozones*; 2017. https://sis.agr.gc.ca/cansis/nsdb/ecostrat/gis data.html (accessed 2022-01-10).
- (36) Brown, J.; Ferrians, O.; Melnikov, E. S. Circum-Arctic Map of Permafrost and Ground-Ice Conditions, Version 2; U.S. Geological Survey 2002.
- (37) Fick, S. E.; Hijmans, R. J. WorldClim 2: New 1-km Spatial Resolution Climate Surfaces for Global Land Areas. *Int. J. Climatol.* **2017**, *37* (12), 4302–4315.
- (38) Hugelius, G.; Loisel, J.; Chadburn, S.; Jackson, R. B.; Jones, M.; MacDonald, G.; Marushchak, M.; Olefeldt, D.; Packalen, M.; Siewert, M. B.; Treat, C.; Turetsky, M.; Voigt, C.; Yu, Z. Large Stocks of Peatland Carbon and Nitrogen Are Vulnerable to Permafrost Thaw. *Proc. Natl. Acad. Sci. U.S.A.* **2020**, *117* (34), 20438–20446.
- (39) Alberta Environment and Sustainable Resource Development. Alberta Wetland Classification System; Water Policy Branch, Policy and Planning Division: Edmonton, AB, 2015. ISBN 978-1-4601-2258-7
- (40) Gibson, C. M.; Cottenie, K.; Gingras-Hill, T.; Kokelj, S. V.; Baltzer, J. L.; Chasmer, L.; Turetsky, M. R. Mapping and Understanding the Vulnerability of Northern Peatlands to Permafrost

- Thaw at Scales Relevant to Community Adaptation Planning. *Environ. Res. Lett.* **2021**, *16* (5), No. 055022.
- (41) Carpino, O.; Haynes, K.; Connon, R.; Craig, J.; Devoie, É.; Quinton, W. Long-Term Climate-Influenced Land Cover Change in Discontinuous Permafrost Peatland Complexes. *Hydrol. Earth Syst. Sci.* **2021**, 25 (6), 3301–3317.
- (42) Estop-Aragonés, C.; Heffernan, L.; Knorr, K.; Olefeldt, D. Limited Potential for Mineralization of Permafrost Peatland Soil Carbon Following Thermokarst: Evidence From Anoxic Incubation and Priming Experiments. *J. Geophys. Res. Biogeosci.* **2022**, *127* (12), No. e2022JG006910.
- (43) Morris, P. J.; Davies, M. L.; Baird, A. J.; Balliston, N.; Bourgault, M.-A.; Clymo, R. S.; Fewster, R. E.; Furukawa, A. K.; Holden, J.; Kessel, E.; Ketcheson, S. J.; Kløve, B.; Larocque, M.; Marttila, H.; Menberu, M. W.; Moore, P. A.; Price, J. S.; Ronkanen, A.-K.; Rosa, E.; Strack, M.; Surridge, B. W. J.; Waddington, J. M.; Whittington, P.; Wilkinson, S. L. Saturated Hydraulic Conductivity in Northern Peats Inferred From Other Measurements. *Water Resour. Res.* **2022**, 58 (11), No. e2022WR033181.
- (44) Riedel, T.; Biester, H.; Dittmar, T. Molecular Fractionation of Dissolved Organic Matter with Metal Salts. *Environ. Sci. Technol.* **2012**, *46* (8), 4419–4426.
- (45) Koch, B. P.; Dittmar, T. From Mass to Structure: An Aromaticity Index for High-Resolution Mass Data of Natural Organic Matter. *Rapid Commun. Mass Spectrom.* **2006**, 20 (5), 926–932.
- (46) Kim, S.; Kramer, R. W.; Hatcher, P. G. Graphical Method for Analysis of Ultrahigh-Resolution Broadband Mass Spectra of Natural Organic Matter, the Van Krevelen Diagram. *Anal. Chem.* **2003**, 75 (20), 5336–5344.
- (47) Mangal, V.; Stock, N. L.; Guéguen, C. Molecular Characterization of Phytoplankton Dissolved Organic Matter (DOM) and Sulfur Components Using High Resolution Orbitrap Mass Spectrometry. *Anal. Bioanal. Chem.* **2016**, *408* (7), 1891–1900.
- (48) Ohno, T.; Sleighter, R. L.; Hatcher, P. G. Comparative Study of Organic Matter Chemical Characterization Using Negative and Positive Mode Electrospray Ionization Ultrahigh-Resolution Mass Spectrometry. *Anal. Bioanal. Chem.* **2016**, 408 (10), 2497–2504.
- (49) Ohno, T.; Ohno, P. E. Influence of Heteroatom Pre-Selection on the Molecular Formula Assignment of Soil Organic Matter Components Determined by Ultrahigh Resolution Mass Spectrometry. *Anal. Bioanal. Chem.* **2013**, *405* (10), 3299–3306.
- (50) Teickner, H.; Hodgkins, S. Irpeat: Simple Functions to Analyze Mid Infrared Spectra of Peat Samples. *Zenodo* **2021**, 10.
- (51) Thompson, L. M.; Olefeldt, D.; Mangal, V.; Knorr, K. H. Soil and Porewater Chemistry from Peatlands of the Interior Plains, Northwestern Canada (Dataset) University of Alberta Education & Research Archive, 2022.
- (52) Hintelmann, H.; Evans, R. D. Application of Stable Isotopes in Environmental Tracer Studies Measurement of Monomethylmercury (CH 3 Hg + ) by Isotope Dilution ICP-MS and Detection of Species Transformation. *Fresenius J. Anal. Chem.* **1997**, 358 (3), 378–385.
- (53) Gionfriddo, C. M.; Wymore, A. M.; Jones, D. S.; Wilpiszeski, R. L.; Lynes, M. M.; Christensen, G. A.; Soren, A.; Gilmour, C. C.; Podar, M.; Elias, D. A. An Improved hgcAB Primer Set and Direct High-Throughput Sequencing Expand Hg-Methylator Diversity in Nature. *Front. Microbiol.* **2020**, *11*, No. 541554.
- (54) Boyd, J. A.; Woodcroft, B. J.; Tyson, G. W. GraftM: A Tool for Scalable, Phylogenetically Informed Classification of Genes within Metagenomes. *Nucleic Acids Res.* **2018**, *46* (10), e59–e59.
- (55) R Core Team. R: A Language and Environment for Statistical Computing, 2024. https://www.R-project.org/.
- (56) Oksanen, J.; Blanchet, F. G.; Kindt, R.; Legendre, P.; Minchin, P. R.; O'Hara, R. B.; Simpson, G. L.; Solymos, P.; Stevens, M. H. H.; Wagner, H. *Vegan: Community Ecology Package. Ver* 2.2–0., 2022. http://CRAN.Rproject.org/package=vegan.
- (57) Fox, J.; Weisberg, S.; Price, B. Car: Companion to Applied Regression, 2001, Ver 3.1-3.

- (58) Lenth, R. V. Emmeans: Estimated Marginal Means, Aka Least-Squares Means, 2017, Ver 1.11.2. .
- (59) McMurdie, P. J.; Holmes, S.; Jordan, G.; Chamberlain, S. Package 'phyloseq', 2017. .
- (60) Olefeldt, D.; Hovemyr, M.; Kuhn, M. A.; Bastviken, D.; Bohn, T. J.; Connolly, J.; Crill, P.; Euskirchen, E. S.; Finkelstein, S. A.; Genet, H.; Grosse, G.; Harris, L. I.; Heffernan, L.; Helbig, M.; Hugelius, G.; Hutchins, R.; Juutinen, S.; Lara, M. J.; Malhotra, A.; Manies, K.; McGuire, A. D.; Natali, S. M.; O'Donnell, J. A.; Parmentier, F.-J. W.; Räsänen, A.; Schädel, C.; Sonnentag, O.; Strack, M.; Tank, S. E.; Treat, C.; Varner, R. K.; Virtanen, T.; Warren, R. K.; Watts, J. D. The Boreal-Arctic Wetland and Lake Dataset (BAWLD). Earth Syst. Sci. Data 2021, 13 (11), 5127–5149.
- (61) Kuhn, M. A.; Olefeldt, D.; Arndt, K.; Bastviken, D.; Bruhwiler, L.; Crill, P.; DelSontro, T.; Fluet-Chouinard, E.; Grosse, G.; Hovemyr, M.; Hugelius, G.; MacIntyre, S.; Malhotra, A.; McGuire, A. D.; Oh, Y.; Poulter, B.; Treat, C.; Turetsky, M. R.; Varner, R. K.; Walter Anthony, K. M.; Watts, J. D.; Zhang, Z. Current and Future Methane Emissions from Boreal-Arctic Wetlands and Lakes. *Nat. Clim. Change* 2025.
- (62) Ecological Stratification Working Group. 1995. A National Ecological Framework for Canada. Agriculture and Agri-Food Canada, Research Branch, Centre for Land and Biological Resources Research and Environment Canada, State of the Environment Directorate, Ecozone Analysis Branch, Ottawa/Hull.
- (63) Tjerngren, I.; Karlsson, T.; Björn, E.; Skyllberg, U. Potential Hg Methylation and MeHg Demethylation Rates Related to the Nutrient Status of Different Boreal Wetlands. *Biogeochemistry* **2012**, *108* (1–3), 335–350.
- (64) Hayashi, M.; Quinton, W. L.; Pietroniro, A.; Gibson, J. J. Hydrologic Functions of Wetlands in a Discontinuous Permafrost Basin Indicated by Isotopic and Chemical Signatures. *J. Hydrol.* **2004**, 296 (1–4), 81–97.
- (65) Quinton, W. L.; Hayashi, M.; Pietroniro, A. Connectivity and Storage Functions of Channel Fens and Flat Bogs in Northern Basins. *Hydrol. Process.* **2003**, *17* (18), 3665–3684.
- (66) Haynes, K. M.; Kane, E. S.; Potvin, L.; Lilleskov, E. A.; Kolka, R. K.; Mitchell, C. P. J. Mobility and Transport of Mercury and Methylmercury in Peat as a Function of Changes in Water Table Regime and Plant Functional Groups. *Global Biogeochem. Cycles* **2017**, 31 (2), 233–244.
- (67) Harris, L. I.; Schulze, C.; Marouelli, K.; Thompson, L.; Shewan, R.; Olefeldt, D. *Greenhouse Gas Flux Data for Peatlands in Northwest Territories and Northern Alberta, 2021* University of Alberta Education & Research Archive, 2025.
- (68) Åkerblom, S.; Nilsson, M. B.; Skyllberg, U.; Björn, E.; Jonsson, S.; Ranneby, B.; Bishop, K. Formation and Mobilization of Methylmercury across Natural and Experimental Sulfur Deposition Gradients. *Environ. Pollut.* **2020**, *263*, No. 114398.
- (69) Schmidt, O.; Hink, L.; Horn, M. A.; Drake, H. L. Peat: Home to Novel Syntrophic Species That Feed Acetate- and Hydrogen-Scavenging Methanogens. *ISME J.* **2016**, *10* (8), 1954–1966.
- (70) Campeau, A.; Amyot, M.; Del Giorgio, P.; Fink-Mercier, C.; Wauthy, M.; Ponton, D. E.; Lapierre, J.-F. Coupling Between Methylmercury and Carbon-Gases Across Boreal Rivers of Québec, Canada. *Geophys. Res. Lett.* **2025**, *52* (14), No. e2025GL115080.
- (71) Yang, Z.; Fang, W.; Lu, X.; Sheng, G.-P.; Graham, D. E.; Liang, L.; Wullschleger, S. D.; Gu, B. Warming Increases Methylmercury Production in an Arctic Soil. *Environ. Pollut.* **2016**, *214*, 504–509.
- (72) Pester, M. Sulfate-Reducing Microorganisms in Wetlands Fameless Actors in Carbon Cycling and Climate Change. *Front. Microbio.* **2012**, *3*, 3.
- (73) Mueller, P.; Megonigal, J. P. Redox Control on Rhizosphere Priming in Wetlands. *Nat. Geosci.* **2024**, *17* (12), 1209–1217.
- (74) Mitchell, C. P. J.; Branfireun, B. A.; Kolka, R. K. Assessing Sulfate and Carbon Controls on Net Methylmercury Production in Peatlands: An in Situ Mesocosm Approach. *J. Appl. Geochem.* **2008**, 23 (3), 503–518.

- (75) Herrero Ortega, S.; Catalán, N.; Björn, E.; Gröntoft, H.; Hilmarsson, T. G.; Bertilsson, S.; Wu, P.; Bishop, K.; Levanoni, O.; Bravo, A. G. High Methylmercury Formation in Ponds Fueled by Fresh Humic and Algal Derived Organic Matter: High Methylmercury Formation in Ponds. *Limnol. Oceanogr.* **2018**, *63* (S1), S44—S53.
- (76) Gandois, L.; Hoyt, A. M.; Hatté, C.; Jeanneau, L.; Teisserenc, R.; Liotaud, M.; Tananaev, N. Contribution of Peatland Permafrost to Dissolved Organic Matter along a Thaw Gradient in North Siberia. *Environ. Sci. Technol.* **2019**, *53* (24), 14165–14174.
- (77) Lei, P.; Nunes, L. M.; Liu, Y.-R.; Zhong, H.; Pan, K. Mechanisms of Algal Biomass Input Enhanced Microbial Hg Methylation in Lake Sediments. *Environ. Int.* **2019**, *126*, 279–288.
- (78) Thompson, L. M.; Low, M.; Shewan, R.; Schulze, C.; Simba, M.; Sonnentag, O.; Tank, S. E.; Olefeldt, D. Concentrations and Yields of Mercury, Methylmercury, and Dissolved Organic Carbon from Contrasting Catchments in the Discontinuous Permafrost Region, Western Canada. *Water Resour. Res.* **2023**, *59*, No. e2023WR034848.
- (79) Shanley, J. B.; Taylor, V. F.; Ryan, K. A.; Chalmers, A. T.; Perdrial, J.; Stubbins, A. Using Dissolved Organic Matter Fluorescence to Predict Total Mercury and Methylmercury in Forested Headwater Streams, Sleepers River, Vermont USA. *Hydrol. Process.* 2022, 36 (5), No. e14572.
- (80) Lin, Y.; Campbell, A. N.; Bhattacharyya, A.; DiDonato, N.; Thompson, A. M.; Tfaily, M. M.; Nico, P. S.; Silver, W. L.; Pett-Ridge, J. Differential Effects of Redox Conditions on the Decomposition of Litter and Soil Organic Matter. *Biogeochemistry* **2021**, *154* (1), 1–15.
- (81) Pracht, L. E.; Tfaily, M. M.; Ardissono, R. J.; Neumann, R. B. Molecular Characterization of Organic Matter Mobilized from Bangladeshi Aquifer Sediment: Tracking Carbon Compositional Change during Microbial Utilization. *Biogeosciences* **2018**, *15* (6), 1733–1747.
- (82) Gilmour, C. C.; Bullock, A. L.; McBurney, A.; Podar, M.; Elias, D. A.; Lovley, D. R. Robust Mercury Methylation across Diverse Methanogenic Archaea. *mBio* **2018**, 9 (2), No. e02403–17.
- (83) Christensen, G. A.; Gionfriddo, C. M.; King, A. J.; Moberly, J. G.; Miller, C. L.; Somenahally, A. C.; Callister, S. J.; Brewer, H.; Podar, M.; Brown, S. D.; Palumbo, A. V.; Brandt, C. C.; Wymore, A. M.; Brooks, S. C.; Hwang, C.; Fields, M. W.; Wall, J. D.; Gilmour, C. C.; Elias, D. A. Determining the Reliability of Measuring Mercury Cycling Gene Abundance with Correlations with Mercury and Methylmercury Concentrations. *Environ. Sci. Technol.* **2019**, 53 (15), 8649–8663.
- (84) Ackley, C.; Tank, S. E.; Haynes, K. M.; Rezanezhad, F.; McCarter, C.; Quinton, W. L. Coupled Hydrological and Geochemical Impacts of Wildfire in Peatland-Dominated Regions of Discontinuous Permafrost. *Sci. Total Environ.* **2021**, *782*, No. 146841.